Final Technical Report for 07HQGR0014 and 07HQGR0008

A Basin Wide Record of Earthquakes at Lake Tahoe: Validation of the Earthquake Induced Turbidite Model with Sediment Core Analysis: Collaborative Research with UNR and SDSU

Principal Investigator: Robert Karlin, University of Nevada, Reno
Co-Principal Investigator: Gordon Seitz, San Diego State University

Abstract

The goal of this project was to characterize and date episodic Holocene turbidites and debris flows in Lake Tahoe to establish an event stratigraphy and determine whether these anomalous deposits were caused by climatic causes or were the result of landslides induced by earthquakes on major faults in the region. Turbidites were correlated and dated in sixteen 3-5 m cores in the lake. Between 14 and 17 events occurred in the last ~11,800 years with an average recurrence interval of ~750 years. Their areal distribution, lithologies, textures and thicknesses suggest that they come from with-in basin landslides along the margins of the lake which have previously been identified by seismic imaging and swath bathymetry. All available evidence suggests that these deposits are due to lake sediment redistribution from catastrophic slope failures, probably seismically-induced rather than from climatic causes such as floods or lake level fluctuations. Additional work is needed to narrow the age ranges and identify specific individual sources.

Introduction

The sediments of Lake Tahoe contain a record of episodic Holocene and Late Pleistocene turbidites and debris flows that can be traced throughout the lake. These disturbances appear to be the result of slope failures and landslides possibly triggered by large magnitude earthquakes along one or more of the faults that pass through the Tahoe basin or nearby range front faults (Figure 1). The turbidite record may then present an unparalleled opportunity to establish a record of strong shaking for the entire Holocene for the region.

The objectives of this project were to 1) validate and date the event stratigraphy and core correlations in the lake; 2) identify probable source areas and the depositional processes responsible for each event; and 3) differentiate seismically induced events from other causes such as lake level fluctuations or floods. The methods developed here can be applied to lacustrine and marine environments in active tectonic settings world-wide. If validated as a shaking record, these results will contribute to the seismic hazard assessment of the Lake Tahoe region by providing a long record of quantifiable strong ground shaking

Twenty-four piston and gravity cores were collected in Lake Tahoe using the UC Davis vessel, the *R/V Laconte*, over the span of several years (Figure 2). Of these, seven piston and three gravity cores were collected in 2006 and studied for the first time during this project. The 3-5 m cores were cut into 1.5 m sections and kept in refrigerated storage at the UNR Core Repository. In the lab, whole core magnetic susceptibility profiles were measured at 1 cm intervals using a Bartington ring sensor. The cores were then split, photographed, and described before sampling. Smear slides were made of representative lithologies. Correlations between cores were established using visual changes in color, texture, and lithology, relative stratigraphic positions, and magnetic susceptibility trends. Prior to this study, only thirteen AMS 14C dates were available from one core, LT00-3, as an initial attempt to establish a chronology.

Investigations Undertaken

Radiocarbon dating

Radiocarbon dating from multiple cores was used to verify the turbidite correlations and to determine the timing and recurrence intervals of episodic events in the lake. Thirty-three new radiocarbon samples from Lake Tahoe were collected from several cores in intervals of 'normal' lacustrine sedimentation. To avoid problems with reservoir ages in sedimentary organic matter, plant macrofossils were isolated and extracted from the bulk material. Dates were run by G. Seitz at the University of Arizona AMS laboratory and at Lawrence Livermore National Laboratory. Thirty-one samples had enough organic material to obtain successful dates for Lake Tahoe (Figure 2; Table 1). Six macrofossil samples from Fallen Leaf Lake also were dated to test whether this nearby small lake could be used as an independent record to compare with Lake Tahoe. Calibrated radiocarbon ages were determined using the program OXCAL v 4.0. All ages are rounded to the nearest fifty years, and are reported with 95% confidence intervals as well as the weighted mean. Weighted means are given in parentheses following age ranges in cal BP. For the best dated core (LT00-2), the top of the core is between 1700 and 1250 cal BP.

In large part, the turbidite correlations were validated by the radiocarbon dating and only a few adjustments to the correlations had to be made. Twenty-one individual events could be correlated within the basin with eighteen events occurring in the Holocene (labeled A to R in Figure 1). Event N was identified by Andrei Sarna-Wojecki as the 7950 to 7750 (7850+/- 50 cal BP, Bacon, 1983) Tsoyowata ash. It occurs between 1.6 and 1.8 m in many of the cores and provides a useful stratigraphic marker. The ash is present as outsized clasts in event M debris flows, often retaining its original bedding. The Holocene turbidites and debris flows vary systematically in thickness indicating their nearness to their source. ^{14}C dates inadvertently obtained from within turbidite intervals showed anomalously old ages, suggesting the presence of reworked organic material. Three events in the latest Pleistocene are not well constrained in age.

The age range of each event was estimated using sequence modeling in OXCAL version 4. A tentative chronology for each event is given in Table 2. The wide uncertainty for many of the events could be greatly improved with further dating. Two intervals have

individual events spaced relatively closely in time (F/G, and K/L) suggesting that they may represent the same disturbance. Events C and D may also be genetically related but as they are found in only one core, the evidence is inconclusive. Recurrence intervals of individual events in Lake Tahoe during the Holocene average about 750 years. In the Holocene, five intervals have repeat times of about 400 to 500 years while longest repeat time is ~1600 years, assuming that C/D. F/G, and K/L are each cogenetic.

The youngest event, A, occurred between 50 and 1200 (550 ± 350) cal BP, which is similar to an age that was obtained for the most recent surface rupture in the Incline Village trench (Seitz, 2005). Event B, between 350 and 1550 (1000 ± 350) cal BP, may be related to the most recent surface rupture on the Mt. Rose fault zone, which is poorly dated (Bell et al., 1984, Ramelli and DePolo, 1997). Event C/D, modeled as a single event, has ages between 1450 and 2500 (2000 ± 300) cal BP and may be related to the penultimate surface rupture on either the Mt. Rose fault zone (Ramelli and DePolo, 1997) or the Genoa fault zone (Ramelli et al., 1999). Event E was dated at between 2400 and 2750 (2600 ± 100) cal BP. This age is within the range estimates associated with the penultimate surface rupture on the Genoa Fault, although it does not fall within the preferred age range of Ramelli et al. (1999). Event H took place between 4050 and 4500 (4300 ± 100) cal BP and is about the same age as the most recent surface rupture on the southern segment of the West Tahoe fault in Fallen Leaf Lake (Brothers et al., 2008). Event I, from 5350 to 5600 cal BP (5500 ± 100) cal BP is about the same age as upright drowned trees found offshore at Baldwin Beach in the southern part of the lake. There remains some controversy about whether the tree drowning was due to lowering of the lake level from tectonic or climatic causes (Lindstrom, 1990). The trees sit on the hanging wall of the West Tahoe fault. The age of the drowned trees also falls within the 95% confidence interval for event J, 5300 to 6600 (5950 ± 350) cal BP. The oldest dated debris flow and turbidite event is between ~12300 and 16950 (14900 ± 1300) cal BP.

Sediment analyses

Detailed sediment analyses were done at 1- to 3-cm intervals on LT00-2, LT00-3, and LT06-1 to characterize the sediment and to develop identifiable tracers of anomalous sedimentation which could be used to assess their cause(s). Grain-size spectra were measured by sieving on the >74 micron fine sand fraction and with a Micromeritics X-ray Sedigraph on the <74 micron fraction. Opal analyses to determine lacustrine diatom content were done using a modified silica extraction technique based on Mortlock and Froelich (1989) and Calvert et al. (2001). Anisotropy of magnetic susceptibility measurements of undisturbed samples were run on an AGICO Kappabridge. Stable isotope (^{13}C and ^{15}N) and total nitrogen and organic carbon percentages were made at the Nevada Stable Isotope Laboratory.

Whole core magnetic susceptibility (WCS) provides a continuous profile of the terrigenous content and to a lesser extent, grain size, within a core. Magnetic susceptibility peaks are associated on a one to one basis with turbidites and debris flows identified visually in the cores. Peak values are highest in the sandy bases of the turbidites. Grain size analyses contain a rich spectrum, but perhaps the easiest way of representing major variations is to simply examine the >74 micron sand fraction (Fig.

3a). In every case, the peaks in this fraction correlate to high values of magnetic susceptibility and define the basal layers of turbidites.

With one exception, biogenic opal from diatoms is diagnostic of 'normal' lacustrine sedimentation. Opal shows an inverse correlation to WCS and coarse grain size (Fig. 3b and 3c). Within the turbidites, basal turbidite layers are largely devoid of diatoms. Diatom content increases through the silty portion of the turbidite. Diatom-rich layers containing numerous fragmented diatom frustrules form the caps of turbidite intervals. These layers are probably deposited as the last fraction that settles out of the turbid cloud due to their lower densities. The presence of opal throughout the turbidites suggests that the turbidites contain reworked lacustrine deposits.

AMS is a measure of the fabric of the deposit and its mode of deposition. Two parameters are often utilized. The 'F' parameter measures the degree of 2-D foliation and gives information about differential stresses during or after deposition. The 'P' parameter indicates the degree of flattening of the susceptibility ellipse, often due to compression. Normal lacustrine sedimentation usually shows values of less than 5% for 'P' and 'F'. The mean sample susceptibility agrees well with the WCS, as would be expected (Figure 4a). However, a significant finding in this study is that the 'F' and 'P' parameters clearly define the turbidite intervals as well as previously unidentified densites (Figure 4b). The downcore increase in 'P' and 'F' from the surface to approximately 100 cm probably reflects compaction as no turbidites are observed in this interval. Within the three major turbidites in this core, peak susceptibilities occur in the basal layer. The 'F' and 'P' parameters show a broader peak in the main body of the turbidite. This is clear evidence that the silty zones above the basal layers are an integral part of the turbidite process. The elevated foliation and flattening are probably due to rapid sediment deposition and compaction. This method could be used in many depositional settings to identify anomalous sedimentation.

Carbon-13 isotopes were examined to distinguish between terrestrial and lacustrine sources of organic sediment into the lake. Opal and $\delta^{13}C$ show a one to one correlation and the largest variations in $\delta^{13}C$ occur within the turbidites (Figure 5a). The $\delta^{13}C$ signal becomes less negative within the turbidite bases indicating a greater amount of terrestrial plant material is present. The $\delta^{13}C$ signal becomes more negative as opal (diatom content) increases throughout the turbidite, grading back to 'normal' lacustrine sedimentation values, which indicate a mix of terrestrial plant material and diatom content. As with the opal, $\delta^{13}C$ reflects grain size sorting as material settles out of the turbid cloud. The terrestrial signal of turbidite bases is the result of the less dense diatoms preferentially settling later, and is not an indicator of a large terrestrial input into the lake.

The nitrogen-15 isotope is also an indicator of organic matter source as well as early diagenesis. Unlike $\delta^{13}C$, $\delta^{15}N$ does not correlate with opal and variations within $\delta^{15}N$ are largely independent of the turbidites (Figure 5b). $\delta^{15}N$ values are all low, indicative of a terrestrial source. This terrestrial signal is expected, as lacustrine sediment is sourced from the material that surrounds the lake. Trends in $\delta^{15}N$ may be representative of diagenesis due to bacterial nutrient usage.

Total organic carbon (TOC), and total nitrogen (TN) may also be representative of organic matter inputs into the lake. TOC and TN correlate to each other on a one to one basis (Figure 5c), which yields a consistent C/N ratio of ~12 throughout the Holocene. Turbidite bases are largely devoid of organic material and have very low TOC and TN abundances. With a given turbidite TOC and TN percentages grade upward into 'normal' lacustrine sedimentation values. Throughout the Holocene, TOC and TN show a general trend of increasing total organic matter input to the lake with time.

Discussion

Detailed stratigraphies of the 2006 cores and the fine-scale sediment analyses on other cores have caused us to revise our paradigm of depositional processes of the anomalous sediments of Lake Tahoe. We now realize that the turbidites are a part of a continuum of gravity flow deposition ranging from slumping (block slumps) to debrites (unsorted debris flows) to densites (turbulent mud/sand flows) to turbidites (sand to silt graded beds sorted during settling)

Debris flows encountered in many of the cores were immediately topped by clearly graded turbidites suggesting that they were rapidly deposited during the same event. The debrites often contained clasts and rip-up beds of reworked lacustrine sediment indicating that the landslides or block slumps cause erosion, deformation, and transport of preexisting lake deposits that are incorporated in the debris flows. Densites consisting of poorly sorted sand to clay are much more difficult to recognize except by AMS as they lack discernable features and in some cases are indistinguishable from 'normal' lacustrine sedimentation. AMS analyses indicate that these deposits represent the transition zone between a debris flows and the overriding turbid cloud.

The graded turbidites range from coarse to fine sand to silt in their basal layers depending on distance to source. The overlying silty layers are graded and the tops are covered by clay and often diatom layers due to density and grain size separation during settling. These deposits can be traced areally based on their relative grain sizes and thicknesses.

Source areas

Source areas for the individual events can be recognized by the presence of proximal debris flows and systematic changes in thickness and grainsize in the more distal turbidites. The debris flows are clear evidence of submarine slope failure and mass redistribution by gravity flow on the lake bottom. Several source areas can be recognized (Figure 6). McKinney Bay is an area in which several landslides are easily identified in the bathymetry (Gardner et al., 2000), and cores around the base of the bay often show evidence of proximal deposits. The northernmost section of the lake around Crystal Bay appears to be proximal to several events, and nearby cores contain numerous debris flows and thick turbidites. The slope off Rubicon Point and the Pleistocene debris apron near Emerald Bay appear to be source areas in the southwestern portion of the lake. Large submarine slumps offshore Zephyr Cove are the sources of debris flows found in several of the nearby cores. Source areas may occur along other parts of the eastern slope, but limited core coverage precludes identification.

All of the Holocene events are associated with debris flows, if C/D, F/G, and K/L are combined (Figure 2). Events I, J, M, O and Q contain debris flows from multiple source areas. Events A, B, and C/D are only identified in one northernmost core, with all 3 events containing a debris flow and thick turbidite, indicative of close proximity to source (Figure 6). Event E is a debris flow and thick turbidite in the northernmost core and contains relatively thick turbidites in the vicinity of central and northern McKinney Bay, suggesting at least two source areas. Event F/G is a debris flow (event G) in the vicinity of southern McKinney Bay and has a relatively thick turbidite in the north central section of the lake (core LT00-1), which also suggests at least two source areas. Event H is a debris flow and turbidite in close proximity to the 'small' landslide seen in the bathymetry just north of McKinney Bay. The youngest of the events with multiple debris flows, event I, contains debris flows and thick turbidites south of McKinney Bay, in central McKinney Bay, in the north-central section of the lake, and in the northernmost part of the lake. This event is also a thick turbidite in northern McKinney Bay. Event J shows a debris flow with a thick overlying turbidite in cores offshore Zephyr Cove and a correlative debris flow across the lake offshore southern McKinney Bay. Thick turbidites associated with this event are present in the northwestern section of the lake as well. Event K/L is a debris flow off southern McKinney Bay, but does not show any noticeable thickness trends within the turbidites. Event M is a massive debris flow topped by a turbidite in all cores from the entire southern end of the lake except one located off the western margin. The event also has thick turbidites in central McKinney Bay. Event O shows debris flows in the northernmost section of the lake and in McKinney Bay, all topped by relatively thicker turbidites. Event P is a debris flow topped by a turbidite in southern McKinney Bay and contains a thicker turbidite in central McKinney bay. Event Q is a debris flow and thick turbidite in central McKinney Bay and in the southern portion of the lake (core LT06-5P). Event R, the oldest of the Holocene events, is part of a debris flow in southern McKinney Bay.

Causes of the debris flows and turbidites

Episodic events in Lake Tahoe may result from tectonic or climatic causes. Strong ground shaking as the result of earthquakes on faults within the region is one way in which large landslides and associated anomalous sediment deposits can occur. Holocene earthquakes have been documented from paleoseismic trenches on several Basin and Range faults in the area. These include the Incline Village fault within the basin and the Genoa and Mt. Rose faults to the east and northeast, respectively. The West Tahoe and North Tahoe faults within the basin are also likely to have had large Basin and Range style offsets in the Holocene. Landslides may be triggered by the initial shock and/or a rise in pore pressure with extended periods of shaking. Hanging wall downdrop on faults within the lake basin could lower lake level and potentially trigger slope destabilization and upper slope landslides in the lake. This would be particularly plausible along the West Tahoe Fault, which stretches along the entire western margin. In addition, gas escape along faults within the basin following large events in the region may lead to slope instability and failure. Pock marks seen in the bathymetry in the southern end of the lake, possibly associated with the West Tahoe fault show that gas release on the basin faults is plausible.

Climatic causes may include storms, flooding, and/or lake level fluctuations. Storms may increase erosion in the watershed and wave-induced erosion along the shoreline. Periodic floods could rapidly introduce large quantities of sediment to the lake, potentially triggering delta collapse and landslides due to oversteepening or pore pressure loading. Changes in lake level could conceivably trigger landslides. Lake level drops during extended periods of drought would cause the upper slope to become exposed, leading to slope instability. Conversely, lake level rises could increase pore pressure leading to slope failure.

Several lines of evidence suggest that debris flow and turbidite deposits in Lake Tahoe are likely to be caused by tectonic processes. Debris flows and turbidites are sourced from areas of submarine landslides, not river or stream sources (Figure 2). Several of the events have multiple source areas, consistent with basin-wide shaking. Rapid deposition and delta collapse due to storms or flooding is not likely, as deltas are not observed (Figure 7). Several streams provide sediment to Lake Tahoe with the main source being the Upper Truckee River, followed by Blackwood Creek, Second Creek, Trout Creek, Third Creek, and Ward Creek (Simon et al., 2003). Most debris flows or turbidites do not appear to originate from the south shore of the lake, which has the largest sediment sources. Large shallow, platforms off south shore, Sugar Pine Point, Tahoe City, and Agate Bay, could potentially provide sediment to the deep lake. However, seismic reflection profiles show that these are relict wave-cut platforms that are bare of sediment accumulation, and thus would not be a major source for turbidites. Most of Lake Tahoe is surrounded by narrow shelves not likely to be sources of sediment accumulation. Further, the debris flows/turbidites have volumes on the order of 10^4 to 10^7 m^3, which is one to four orders of magnitude greater than the annual sediment input via the Upper Truckee River and up to 3 orders of magnitude greater than the average annual total sediment load to Lake Tahoe.

Sedimentological studies indicate that turbidites and debris flows contain significant fractions of reworked lacustrine sediment. Debris flows contain clay balls and outsized lacustrine clasts. Turbidites show strong effects of grain size sorting, with coarse terrigenous material toward the base and high abundances of diatom-derived opal and more negative $\delta^{13}C$ in the overlying fining upward sequence. This suggests that the debris flows and turbidites are sourced within the lake, which is consistent with seismically induced landslides causing sediment deformation and redistribution.

Major findings from this study

- Recurrence intervals of debris flow and turbidite events in Lake Tahoe during the Holocene average about 750 years. In the Holocene, five intervals have repeat times of about 400 to 500 years while longest repeat time is ~1600 years. The most recent event occurred 550 ± 350 cal BP.

- Events A-E may correlate to surface ruptures on the Incline Village fault, the Mt. Rose fault, and the Genoa Fault. Event H correlates to the most recent surface rupture on the southern segment of the West Tahoe fault in Fallen Leaf Lake.

- Detailed stratigraphies and sediment analyses suggest that events in Lake Tahoe represent a continuum of processes sourced within the lake, from submarine landslides to lacustrine debris flows to densites to turbidites.

- Source areas for individual events and detailed sediment analyses, indicate debris flows and turbidites are initiated within the lake as the result of submarine landslides, consistent with strong shaking on faults within the basin, the West Tahoe, North Tahoe, and Incline Village faults, and on nearby faults, the Mount Rose fault zone and the Genoa fault zone.

Future work

Additional dating is needed in order to refine ages of individual events throughout the cores and better correlate the younger events, which are most feasible to be linked to fault trench studies. Age ranges for many of the events are not currently well constrained and consequently recurrence intervals have a large uncertainty. Some cores also contain young events which cannot be readily correlated within the basin without better age control. Better age constraints would also improve estimates of landslide volumes and allow the events to be more closely tied to surface ruptures observed elsewhere. Additional dating would allow us to determine if events F and G and events K and L are cogenetic or separate, but clustered events.

Additional cores are needed to better identify and characterize the sources, areal extent, and volume of debris flow and turbidites and to tie events into individual slides. The spatial distribution of debris flow and turbidite events is not well constrained along the eastern margin. Piston coring often results in the loss of the uppermost section of sediment (most cores are ~2200 years cal BP at the top). Gravity cores would provide a more complete record to identify the uppermost debris flows and turbidites, which are currently only found in one core. Additional gravity cores would allow us to better date these uppermost events, as well as to determine whether event C and D are co-genetic or separate.

The results of this study have been reported in three abstracts at the American Geophysical Union and the Geological Society of America annual meetings in 2006 and 2007. One paper on Fallen Leaf Lake is in review in the Bulletin of the Seismological Society of America and three major papers are in preparation and should be submitted by the end of this year.

Published abstracts and papers submitted

Brothers, D.S., Kent, G.M., Driscoll, N.W., Smith, S.B., Seitz, G.G., Dingler, J.A., Karlin, R., Harding, A.J., Babcock, J.M., 2008, Late Pleistocene-Holocene earthquake history and slip-rate estimates for the West Tahoe, Dollar Point Fault, Lake Tahoe Basin, California, Bulletin of the Seismological Society of America, in review.

Smith, S.B., Karlin, R., Seitz, G., Kent, G., 2007, Clastic sedimentation in Lake Tahoe as a record of submarine landsliding and seismic shaking, Eos Trans. AGU, 88 (52), Fall Meet. Suppl., Abstract OS33A-1000

Smith, S.B., Karlin, R., Seitz, G., Kent, G., 2006, Earthquake-induced submarine landslides in Lake Tahoe, 87 (52), Fall Meet. Suppl., Abstract OS43C-0667

Smith, S.B., Karlin, R., Seitz, G., Kent, G., 2006, Seismically-induced landslides, debris flows, and turbidites in Lake Tahoe, Geological Society of America Abstracts with Programs, Vol. 38, No. 7, p. 549

References:

Bacon, C.R., 1983, Eruptive history of Mount Mazama and Crater Lake caldera, Cascade Range, U.S.A: Journal of Volcanology and Geothermal Research, v. 18 p. 57-115 doi: 10.1016/0377-0273(83)90004-5.

Bell, J.W., Slemmons, D.B., and Wallace, R.A., 1984, Reno to Dixie Valley-Fairview Peak earthquake areas, in Lintz, J., Jr., ed., Western geological excursions: Reno, Nevada, University of Nevada, Mackay School of Mines, 1984 Annual Meetings of the Geological Society of America, Guidebook, v. 4, p. 425-472.

Brothers, D.S., Kent, G.M., Driscoll, N.W., Smith, S.B., Seitz, G.G., Dingler, J.A., Karlin, R., Harding, A.J., Babcock, J.M., 2008, Late Pleistocene-Holocene earthquake history and slip-rate estimates for the West Tahoe, Dollar Point Fault, Lake Tahoe Basin, California, Bulletin of the Seismological Society of America, in review.

Calvert, S.E., Pedersen, T.F., and Karlin, R.E., 2001, Geochemical and isotopic evidence for post-glacial palaeoceanographic changes in Saanich Inlet, British Columbia, Marine Geology, v. 174, p. 287-305.

Gardner, J. V., Mayer, L. A., and Hughs Clarke, J. E., 2000, Morphology and processes in Lake Tahoe (California-Nevada): Geological Society of America Bulletin, v. 112, no. 5, p. 736-746.

Lindstrom, S., Submerged tree stumps as indicators of Mid-Holocene aridity in the Lake Tahoe Basin, 1990, Journal of California and Great Basin Anthropology, v. 12, p. 146-147.

Mortlock, R.A., and Froelich, P.N., 1989, A simple method for the rapid determination of biogenic opal in pelagic marine sediments, Deep Sea Research, v. 36, no. 9, p. 1415-1426

Ramelli, A. R., Bell, J.W., dePolo, C.M., and Yount, J.C., 1999 Large-magnitude, late Holocene earthquakes on the Genoa fault, west-central Nevada and eastern California, Bulletin of the Seismological Society of America, v. 89, p. 1458-1472.

Ramelli, A.R., and dePolo, C.M., 1997, Trench and related studies of the northern Sierra Nevada Range-front fault system: National Earthquake Hazards Reduction Program, Final Technical Report, 21 p., scale 1:62,500.

Seitz, G.G., Kent, G., Dingler, J., Karlin, R., Babcock, J., Driscoll, N., and Turner, R., 2005, First paleoseismic results from the Lake Tahoe Basin: Evidence for three M7 range earthquakes on the Incline Village fault: Seismological Society of America, Annual Meeting, 2005.

Simon, A., Langendoen, E, Bingner, R., Wells, R, Heins, A., Jokay, N, and Jaramillo, I, 2003, Lake Tahoe Basin Framework Implementation Study: Sediment Loadings and Channel Erosion, USDA ARS Technical Report

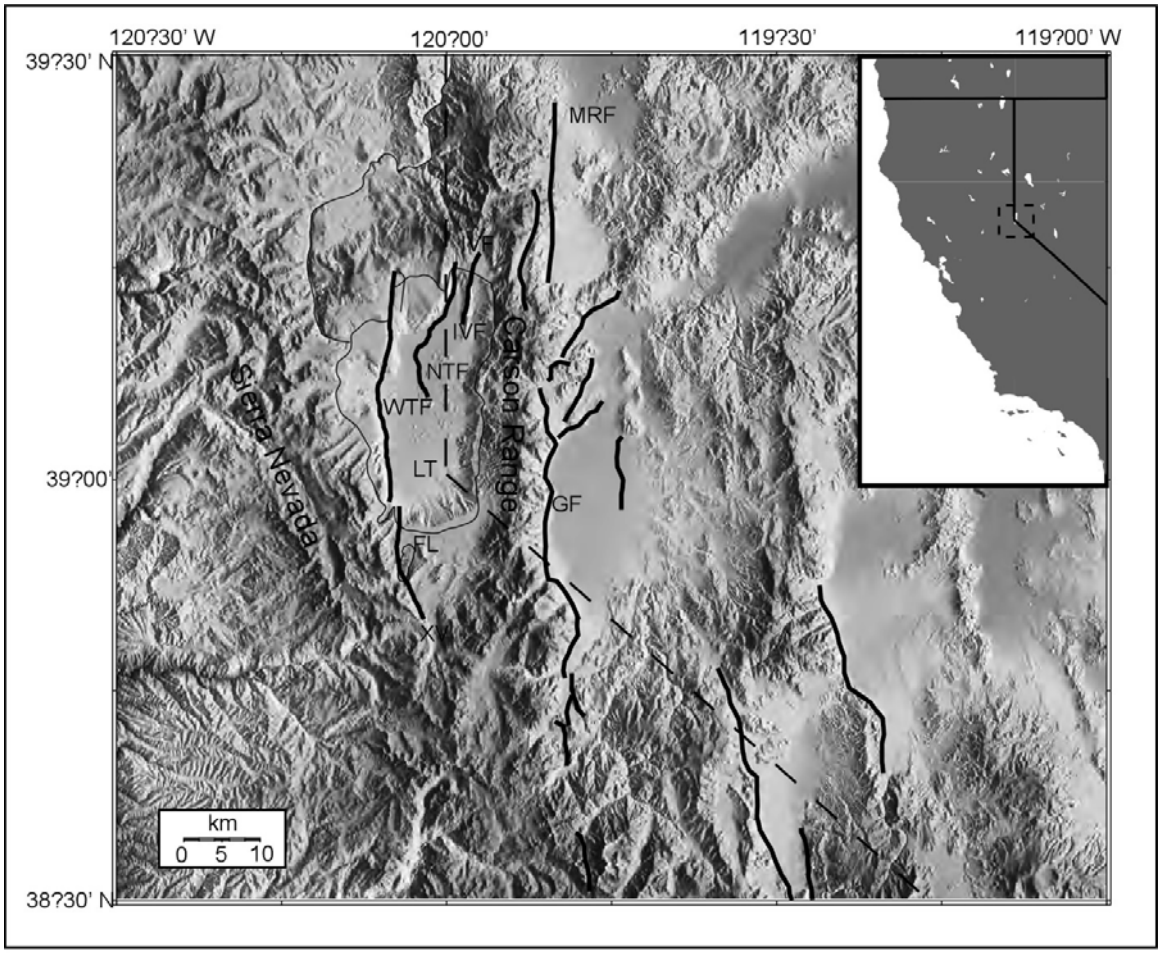

Figure 1: Location map of Lake Tahoe (LT), Fallen Leaf Lake (FL), and selected faults in the region; the West Tahoe Fault (WTF), the North Tahoe Fault (NTF), and the Incline Village Fault (IVF) in the basin, and the Genoa Fault (GF) and the Mount Rose Fault (MRF) to the east of the basin (modified from Brothers et al., 2008, Fig. 1).

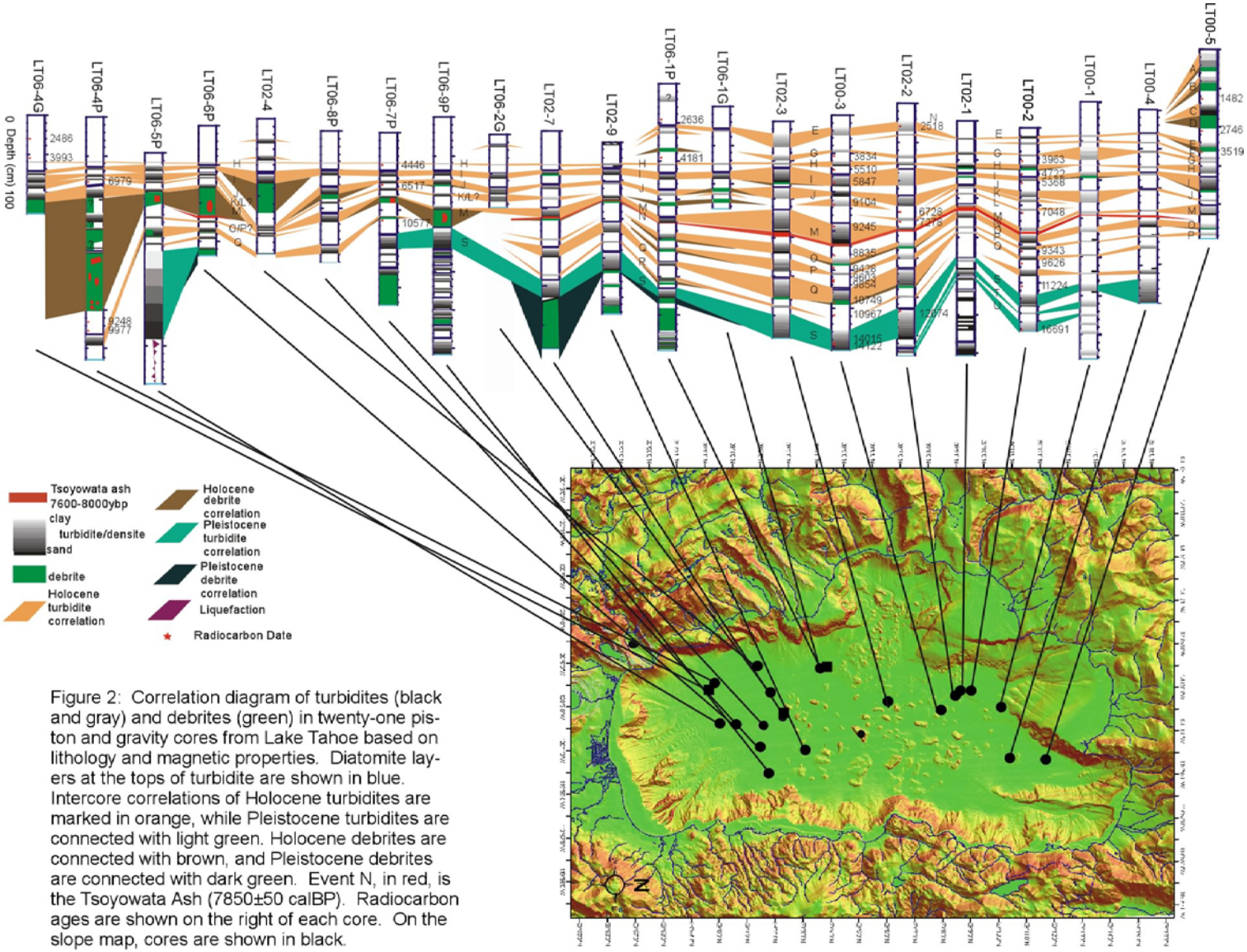

Figure 2: Correlation diagram of turbidites (black and gray) and debrites (green) in twenty-one piston and gravity cores from Lake Tahoe based on lithology and magnetic properties. Diatomite layers at the tops of turbidite are shown in blue. Intercore correlations of Holocene turbidites are marked in orange, while Pleistocene turbidites are connected with light green. Holocene debrites are connected with brown, and Pleistocene debrites are connected with dark green. Event N, in red, is the Tsoyowata Ash (7850±50 calBP). Radiocarbon ages are shown on the right of each core. On the slope map, cores are shown in black.

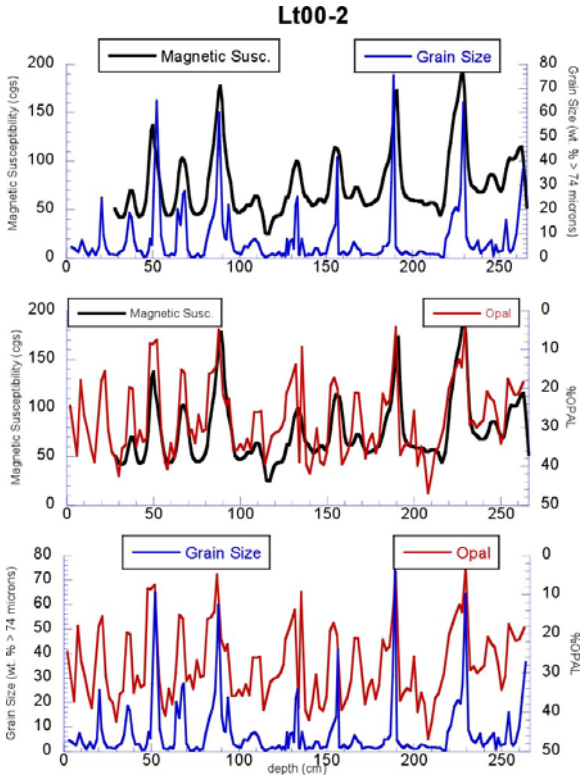

Figure 3: Whole core magnetic susceptibility (black), grain size (blue), and %OPAL (red) for core LT00-2 are plotted vs. depth. Note that the %OPAL scale has been reversed in B and C. A.) Whole core magnetic susceptibility and grain size vs. depth. B.) Whole core magnetic susceptibility and %OPAL vs. depth. C.) Grain size and %OPAL vs. depth.

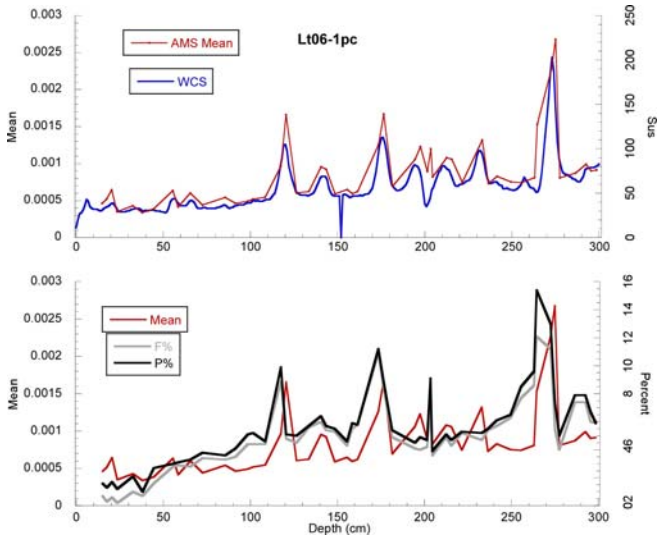

Figure 4: Anisotropy of magnetic susceptibility (AMS) for core LT06-1 vs. depth. A.) Whole core magnetic susceptibility (blue) and mean susceptibility from AMS (red) vs. depth. B. Mean susceptibility from AMS (red), magnetic foliation (F%, gray), and degree of flattening (P%, black) vs. depth.

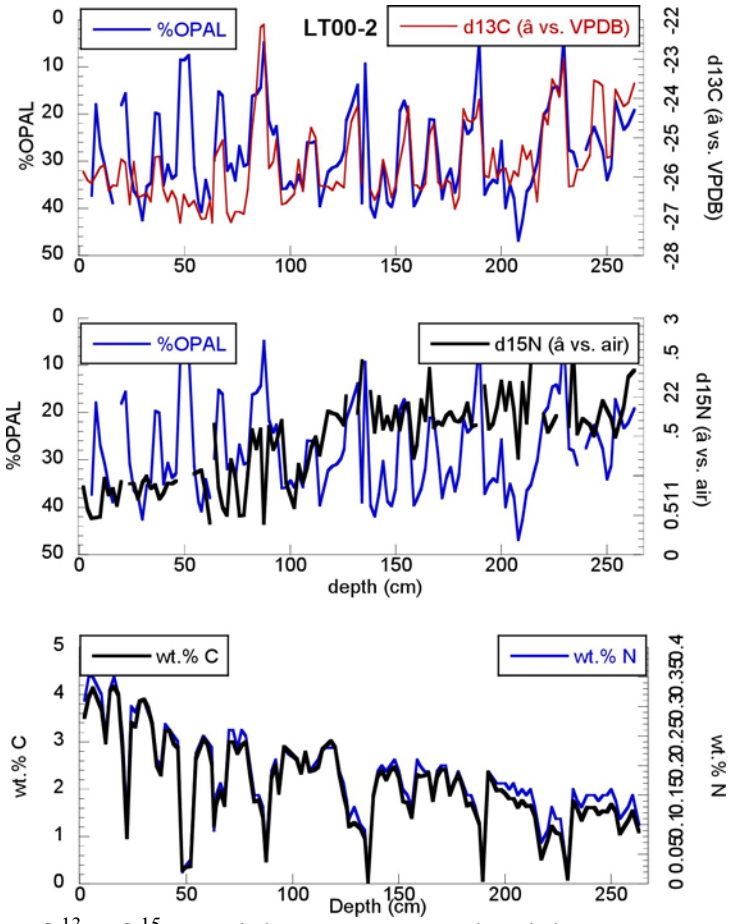

Figure 5: %OPAL, $\delta^{13}C$, $\delta^{15}N$, weight percent C, and weight percent N vs. depth for core LT00-2. A.) %OPAL and $\delta^{13}C$ vs. depth. B.) %OPAL and $\delta^{15}N$ vs. depth. C.) Weight percent carbon and weight percent nitrogen vs depth.

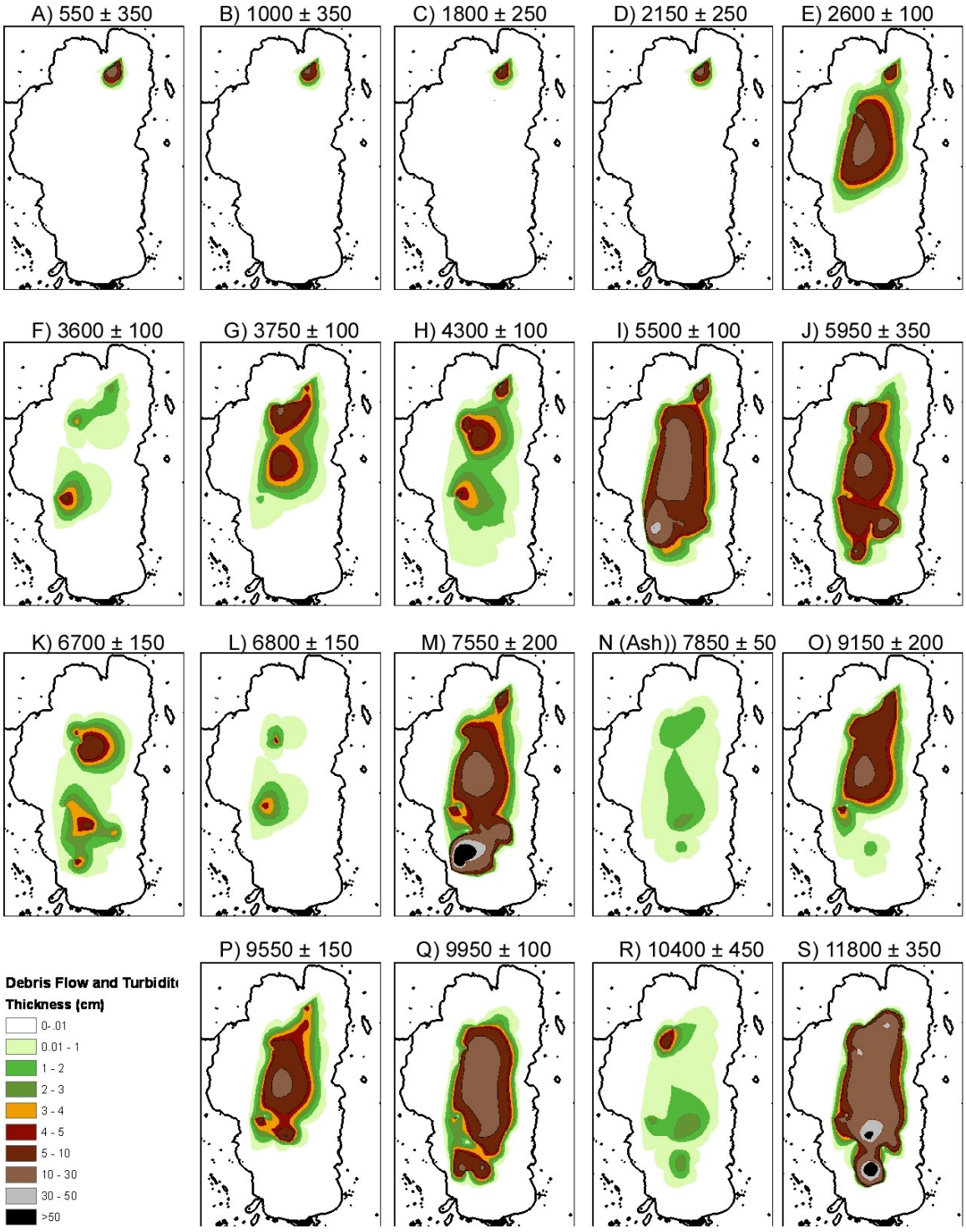

Figure 6: Debris flow and turbidite thicknesses for events A-S with modeled weighted mean ages in cal BP.

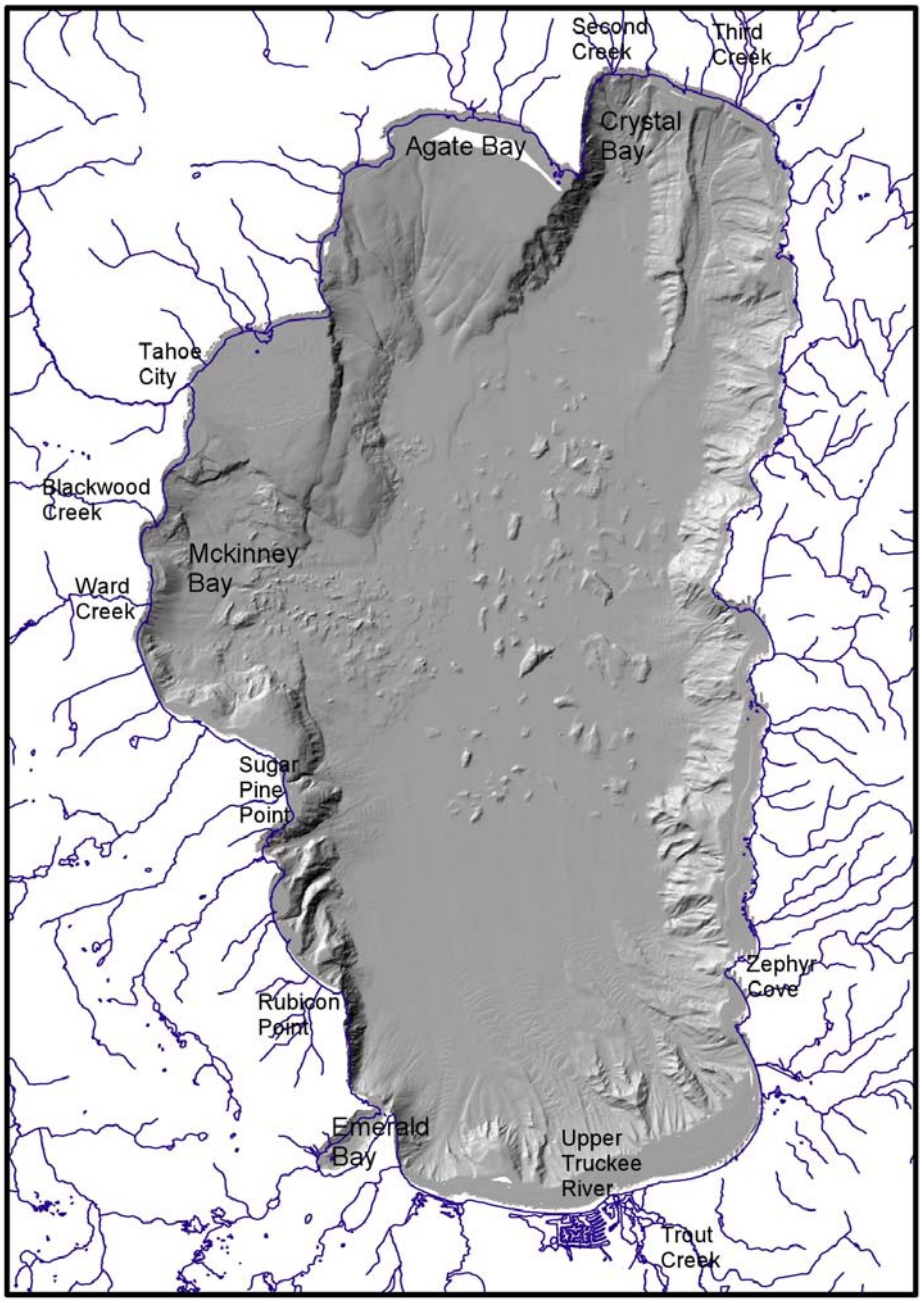

Figure 7: Lake Tahoe bathymetry (Gardner et al., 2000), surrounding streams, and locations noted in the text.

Table 1: Radiocarbon samples and dates. AA lab numbers are from Arizona, others are from LLNL. Ranges in cal BP are at the 95%confidence interval.

Lab #	Sample Name	^{14}C age	error	Range from (cal BP)*	Range to (cal BP)	Mean (cal BP)	error	Sample Type
AA76346	LT00-2-40-44	3630	120	4350	3650	3950	150	macrofossil
AA76347	LT00-2-60-62	4189	39	4850	4600	4700	50	macrofossil
AA76348	LT00-2-69-71	4660	100	5600	5050	5350	150	macrofossil
AA76349	LT00-2-108-110	6160	110	7300	6750	7050	150	macrofossil
AA76350	LT00-2-159-161	8350	360	10250	8450	9350	450	macrofossil
AA76351	LT00-2-173-175	8590	110	10100	9300	9650	150	macrofossil
AA76352	LT00-2-204	9804	53	11300	11150	11200	50	macrofossil
AA76353	LT00-2-261-262.5	13990	170	17300	16100	16700	300	macrofossil
AA76354	LT06-1p-48	2549	37	2750	2500	2650	100	macrofossil
AA76355	LT06-1p-96	3790	100	4450	3900	4200	150	macrofossil
AA76356	LT02-2-140	5880	180	7150	6300	6750	200	macrofossil
AA76357	LT02-2-151	6400	190	7650	6900	7300	200	macrofossil
AA76358	LT02-2-28	2440	120	2750	2150	2500	150	macrofossil
AA76360	LT02-2-267	10320	280	12800	11250	12050	450	macrofossil
AA76362	LT06-7p-41	3976	44	4550	4300	4450	50	macrofossil
AA76363	LT06-7p-67	5710	110	6750	6300	6500	100	macrofossil
AA76364	LT06-7p-114	9357	51	10700	10400	10600	50	macrofossil
AA76366	LT06-4g-30	2421	36	2700	2350	2500	100	macrofossil
AA76367	LT06-4g-57	3661	38	4150	3900	4000	50	macrofossil
AA76368	LT06-4p-83	6095	79	7150	6750	7000	100	macrofossil
AA76369	LT06-4p-268	8263	66	9450	9050	9250	100	macrofossil
AA76370	LT06-4p-278	8861	50	10150	9750	10000	100	macrofossil
AA76371	FLL06-p3-190	3580	110	4250	3600	3900	150	macrofossil
AA76374	FLL06-p3-383	4235	44	4850	4600	4800	50	macrofossil
AA76375	FLL06-p3-340	5506	41	6400	6200	6300	50	macrofossil
AA76376	FLL06-p5-236	6003	48	7000	6750	6850	50	macrofossil
AA76379	LT00-5-131	3290	38	3650	3400	3500	50	macrofossil
AA76365	LT06-4g-7	***	***	***	***	***	***	macrofossil
128008	FF06P3CC	4795	45	5600	5350	5500	50	macrofossil
128009	FF06P4CC	7995	40	9000	8650	8850	100	macrofossil
N80085	LT00-5-32cm	***	***	***	***	***	***	macrofossil
N80086	LT00-5-62cm	1605	35	1550	1400	1500	50	macrofossil
N80087	LT00-5-106cm	2515	40	2750	2450	2600	100	macrofossil
69874	LT00-3-52	3550	50	3950	3700	3850	100	macrofossil
73700	LT00-3 73	4780	40	5600	5350	5500	50	macrofossil
69875	LT00-3-87.5/88.5	5120	50	6000	5750	5850	50	macrofossil
69876	LT-00-3-118	8140	60	9300	8800	9100	100	macrofossil
69877	LT00-3-145.5	8260	40	9400	9100	9250	100	macrofossil
69878	LT00-3-182	7970	50	9000	8650	8850	100	macrofossil
73701	LT00-3 199	8410	50	9500	9300	9450	50	macrofossil
73702	LT00-3 215	8780	130	10200	9550	9850	200	macrofossil
73704	LT00-3 215*	8550	230	10200	9050	9600	300	humics
69879	LT00-3-241.5	9460	60	11050	10550	10750	150	charcoal
73703	LT00-3 260	9600	250	11750	10250	10950	400	humics
69880	LT00-3-297.5	12160	40	14150	13900	14000	50	macrofossil
69881	LT00-3-297.5*	12200	110	14600	13800	14100	200	humics

Table 2: Modelled ages of debris flow/turbidite events. Age ranges are at the 95% confidence interval.

Event	Weighted Mean (cal BP)			Range (cal BP)	
				from	to
A	550	±	350	1200	50
B	1000	±	350	1500	350
C	1800	±	250	2300	1450
D	2150	±	250	2600	1650
E	2600	±	100	2750	2400
F	3600	±	100	3800	3450
G	3750	±	100	3900	3550
H	4300	±	100	4500	4050
I	5500	±	100	5600	5350
J	5950	±	350	6600	5300
K	6700	±	150	7000	6400
L	6800	±	150	7050	6500
M	7550	±	200	7900	7200
N (Ash)	7850	±	50	7950	7750
O	9150	±	200	9450	8800
P	9550	±	150	9800	9300
Q	9950	±	100	10150	9800
R	10400	±	450	11200	9600
S	11800	±	350	12500	11200
T	13100	±	1300	15600	11200
U	14900	±	1300	17000	12300

OXCAL v. 4.0